Molecular Dynamics Study of Polymer−Water Interaction in Hydrogels. 1. Hydrogen-Bond Structure

Yoshinori Tamai* and Hideki Tanaka

Department of Polymer Chemistry, Graduate School of Engineering, Kyoto University, Kyoto 606-01, Japan

Koichiro Nakanishi

Department of Chemical Technology, Kurashiki University of Science and the Arts, Nishinoura 2640, Tsurajima-cho, Kurashiki, Okayama 712, Japan

Received October 31, 1995; Revised Manuscript Received July 1, 1996[⊗]

ABSTRACT: Molecular dynamics simulations have been performed for hydrogel models of poly(vinyl alcohol) (PVA), poly(vinyl methyl ether) (PVME), and poly(*N*-isopropylacrylamide) (PNiPAM). The spatial distributions and stability of hydrogen bonds in the vicinity of polymer segments are analyzed to investigate the properties of water which is highly cooperative with the surrounding polymer chains. Water−water hydrogen bonds are enhanced around hydrophobic groups especially for PVME and PNiPAM by the hydrophobic hydration. Hydrogen bonds are also stabilized around hydrophilic groups for PVME and PNiPAM. The stabilization is accounted for by a severe constraint of the mutual orientation between water and polar group.

Introduction

Investigation on mixtures of polymers and water from a microscopic viewpoint is very important in both scientific and technological fields. The properties of polymer materials depend seriously on the degree of the moisture sorption. The phenomena such as the moisture permeation in membranes, the sorption of water in hydrogels, the wetting in interfaces, etc., have a close relation to realization of various properties of polymers as functional materials. Investigation on the mixtures of polymers and water is also helpful to the molecular design of functional separation membranes and understanding the mechanism of the plasticization of polymers. This also contributes to understanding structure and dynamics of polymers with other small molecules when comparison is made.

The hydrogels, which are made of hydrophilic polymer and water, are used for various functional materials. The hydrogels which have the lower critical solution temperature (LCST) swell at low temperature and are transformed into condensed state by the volume phase transition at high temperature. These hydrogels are supposed to be used for intelligent materials which respond sensitively to temperature. The interaction between water and polymers seems to play an essential role in this transition. Water molecules in the hydrogels have different properties from those of pure water since those are constrained by polymers. It is very interesting to study some characteristics of water molecules coexisting with hydrophilic polymers, because it has some relation to the folding of proteins and various biological phenomena.

Water has anomalous physicochemical properties due to three-dimensional hydrogen-bond networks. These days, the physicochemical properties of water are elucidated by many molecular simulation studies using molecular dynamics (MD) or Monte Carlo (MC) methods.[1] It has been well recognized that hydrogen bonds play a significant role in those anomalous static and dynamic properties of water. Various attempts have also been made to explore the effects of hydrogen-bond networks on mobility and various properties of water and aqueous solutions.[2] Ladanyi and Skaf have reviewed computer simulation of hydrogen-bonding liquids extensively.[3]

As for interaction between water and polymers, analyses have been made for hydration structure of proteins by MD simulation. For example, Kitao et al.[4,5] investigated the effects of solvent on the conformation and collective motions of a protein molecule. Water molecules are highly influenced in the presence of polymer chains. Terada et al.[6] evaluated the number of hydrogen-bond defects caused by a monomer unit of synthetic polymer gels by measuring the relative intensities of collective bands in the Raman spectroscopy. The numbers of defects of water in hydrophilic polymer solutions are greater than those in hydrophobic polymer solutions. Maeda et al.[7] evaluated the dependence of the number of defects on the molecular weights and the degrees of cross-links of polymers. They found that the numbers of defects increase with increasing the molecular weights and the degrees of cross-links. They argued that the number of defects increases when the size of the cluster of *interstitial water* surrounded by polymer networks decreases below a critical size and the orientation of water molecules is restricted.

Poly(vinyl alcohol) (PVA) is soluble in water at high temperature but is insoluble at low temperature. On the other hand, poly(vinyl methyl ether) (PVME) and poly(*N*-isopropylacrylamide) (PNiPAM) are soluble in water at low temperature but are not soluble, and phase separations are observed at high temperature: PVME and PNiPAM have LCST. The difference in solubility arises necessarily from a difference in the interaction between water and polymers. Ohta et al.[8] measured the mobility of water molecules in the PNiPAM solution around the volume phase transition temperature by the spin−spin relaxation time T_2 in NMR. In the pure water, T_2 increases linearly with temperature. Though T_2 in the PNiPAM solution increases with temperature in most of the temperature range, it decreases discontinuously at the phase transition temperature, at which the mobility of water molecules is significantly depressed. It is generally accepted that the volume phase transition phenomenon has a close relation to the change of the entropy of water caused by the hydrophobic effect.

[⊗] Abstract published in *Advance ACS Abstracts,* September 1, 1996.

S0024-9297(95)01635-4 CCC: $12.00

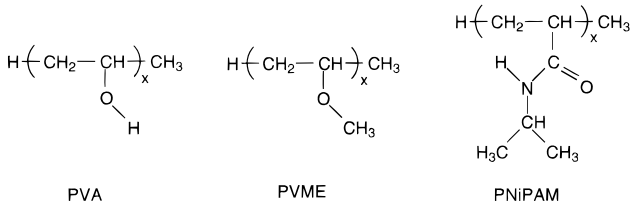

Figure 1. Structures of poly(vinyl alcohol) (PVA), poly(vinyl methyl ether) (PVME), and poly(*N*-isopropylacrylamide) (PNiPAM).

Table 1. Samples of Hydrogels[a]

polymer	x	n_w	c_w (wt %)
	$c_w \simeq 0$ wt %		
PVA	161	5	0.25
	$c_w \simeq 25$ wt %		
PVA	161	150	27.54
PNiPAM	81	150	22.74
	$c_w \simeq 50$ wt %		
PVA	81	199	50.00
PVME	81	199	43.16
PNiPAM	4	199	43.50
	$c_w \simeq 75$ wt %		
PVA	21	215	79.72
PVME	21	215	74.96
PNiPAM	11	215	75.44

[a] x, n_w, and c_w are degree of polymerization, number of water molecules in a unit cell, and water content, respectively.

In this study, we have performed MD simulations for the hydrogel models of PVA, PVME, and PNiPAM with various water contents under several temperature conditions to elucidate the interaction between water and polymers. In our preliminary study,[9] the distribution of hydrogen bonds was analyzed for aqueous solutions of PVA, PVME, and PNiPAM through MD simulations. Further analyses are made on the distribution and dynamics of hydrogen bonds, and the translational and rotational motions of water, with directing our attention mainly to water molecules. These properties are expected to depend significantly on the surrounding polymer matrices. In this article, equilibrium results, structure and stability of hydrogen-bond networks, are presented. The dynamics will be discussed in an accompanying paper.[10]

Model and Simulation Details

Model and Potential Functions. The primary structures of PVA, PVME, and PNiPAM are shown in Figure 1. Polymer samples of water contents 0, 25, 50, and 75 wt % are generated and used as hydrogel models. Table 1 lists the water content c_w, the degree of polymerization x, and the number of water molecules n_w of the systems simulated. The tacticity of all the main chains is set to be atactic. Sequences of monomer units of *d*- and *l*-structures are generated randomly with constraining the fraction of meso diads to 0.5.

The AMBER/OPLS[11] force field is used for the polymers, and the SPC/E[12] for water. The united atom approximation is applied for $-CH_3$, $-CH_2-$, and $>CH-$ groups, each of which is treated as a single interaction site. The potential energy of the system is described as

$$V = \sum k_b(l - l_0)^2 + \sum k_\theta(\theta - \theta_0)^2 + \sum k_\phi[1 + \cos(n\phi - \delta)] + \sum_{i<j}\left(\frac{A_{ij}}{r_{ij}^{12}} - \frac{C_{ij}}{r_{ij}^{6}}\right) + \sum_{i<j}\frac{q_i q_j}{4\pi\varepsilon_0 r_{ij}} \quad (1)$$

Table 2. Nonbonded Potential Parameters[a]

atom	ϵ	σ	q	m
		PVA		
CH_3	0.669 89	3.9100	0.0	15.0350
CH_2	0.494 04	3.9050	0.0	14.0270
CH	0.334 94	3.8500	0.265	13.0190
O (alcohol)	0.711 76	3.0700	−0.70	15.9994
H (alcohol)	0.0	0.0	0.435	1.0080
		PVME		
CH_3 (end)	0.669 89	3.9100	0.0	15.0350
CH_2	0.494 04	3.9050	0.0	14.0270
CH	0.334 94	3.8500	0.25	13.0190
O (ether)	0.711 76	3.0000	−0.50	15.9994
CH_3 (side)	0.711 76	3.8000	0.25	15.0350
		PNiPAM		
CH_3 (end)	0.669 89	3.9100	0.0	15.0350
CH_2	0.494 04	3.9050	0.0	14.0270
CH	0.334 94	3.8500	0.0	13.0190
C (amide)	0.439 61	3.7500	0.50	12.0110
O (amide)	0.879 23	2.9600	−0.50	15.9994
N (amide)	0.711 76	3.2500	−0.57	14.0067
H (amide)	0.0	0.0	0.37	1.0080
CH (side)	0.334 94	3.8000	0.20	13.0190
CH_3 (side)	0.669 89	3.9100	0.0	15.0350
		SPC/E water		
O	0.6502	3.1656	−0.8476	15.9994
H	0.0	0.0	0.4238	1.0080

[a] Energies are in kJ/mol, distances in Å, charges in esu, and masses in g/mol.

where l is the bond length, θ is the bond angle, ϕ is the dihedral angle, k_b, k_θ, and k_ϕ are the force constants, l_0 is the equilibrium bond length, θ_0 is the equilibrium bond angle, n is the multiplicity factor, and δ is the phase shift. In the AMBER force field,[13] the dihedral angle potential function is also used to describe the improper torsion angle potential, which ensures planarity of the sp^2 bond and prevents transitions from *d*- to *l*-structures and vice versa when the united atom approximation is used for chiral $>CH-$ groups. The last two terms of eq 1 are nonbonded potential functions, where r_{ij} is the distance between atom i and j, and A_{ij} and C_{ij} are coefficients arising from the Lennard-Jones interaction parameters, represented by $A_{ij} = (A_{ii}A_{jj})^{1/2}$, $C_{ij} = (C_{ii}C_{jj})^{1/2}$, $A_{ii} = 4\epsilon_i\sigma_i^{12}$, and $C_{ii} = 4\epsilon_i\sigma_i^{6}$, where ϵ and σ are energy and size parameters of the Lennard-Jones potential. The last term is the Coulomb potential, where q_i is the charge of atom i and ε_0 is the dielectric constant of vacuum.

The original potential parameters of the AMBER[13] are used for intramolecular interaction except two parameters. The bond angle parameters for $CH_2-CH-CH_3$ and CH_2-O-CH_3 are substituted for $CH_2-CH-CH_2$ and $CH-O-CH_3$, respectively, because the latter parameters are not defined in the original AMBER force field. The OPLS[11] force field, which is parametrized to reproduce thermodynamic properties of small molecules, is used for intermolecular interactions. Table 2 lists the Lennard-Jones interaction parameters ϵ and σ, the partial charge q, and the mass weight m on each atom type. Only the Lennard-Jones and Coulomb terms are included in the SPC/E water. A detailed description of the potential functions is given elsewhere.[15]

Calculations are performed on NEC SX-3 and CRAY Y-MP2E supercomputers and HP-9000 700-series workstations, using the molecular simulation program PAMPS we coded.

Generation of Initial Structures. Using the modified self-avoiding random walk method, a single polymer chain is confined in a unit cell under the periodic

boundary condition at 300 K. In this method, a chain is built up site by site with fixed bond lengths and bond angles and with randomly generated dihedral angles. After evaluating the energy of a new dihedral angle and also the energy between a new site and already settled atoms, the site is either accepted or rejected by the Monte Carlo method similar to the Metropolis scheme. If one site is rejected repeatedly, the chain is shortened and another route to growth is searched for. After the position is accepted, dihedral angles for the atoms of the subsequent chain are generated successively. The initial density is 0.01 g/cm^3, at which the chains cannot interact with the image chains.

After the steepest-descent energy minimization, MD simulations are performed; at this stage velocities of atoms are scaled at regular intervals to keep temperature. The equations of motion are solved by the Verlet algorithm[16] with a time step of 0.5 fs. The bond angles, H−O−H of water and CH−O−H of PVA, and all the bond lengths are constrained by the SHAKE algorithm.[17,18] Simulations are performed at high temperature, 400 K, to speed up equilibration of the polymer conformation. A simulation of 10 000 steps is performed at initial density. Then, the unit cell is compressed to a density of 0.1 g/cm^3. After the steepest-descent energy minimization, a simulation of 10 000 steps is performed. A further simulation is performed for 10 000 steps, compressing the unit cell toward a density of 0.25 g/cm^3 step by step. An equilibration run of 50 000 steps is performed at the fixed density. The alternate compression and equilibration runs produce the equilibrium structures of the densities of 0.25, 0.5, 0.75, 1.0, and 1.25 g/cm^3.

Since the Coulomb potentials are too strong, polymer chains without explicit water molecules cohere at low density condition when using the dielectric constant in vacuum. To implicitly incorporate the screening effect on the Coulomb potential by water, the distance dependent dielectric constant $\varepsilon(r)$ is used at this stage, instead of ε_0 in eq 1.

$$V_C = \sum_{i<j} \frac{q_i q_j}{4\pi\varepsilon(R_{ij}) r_{ij}} S(R_{ij}) \tag{2}$$

where R_{ij} is the distance between the center of mass of the neutral group to which atom i belongs and that to which atom j belongs. Distances between the groups in a unit of Å are used for the relative dielectric constants.[13]

$$\varepsilon(R) = \varepsilon_0 R \tag{3}$$

The switching function

$$S(r) = \begin{cases} 1 & r \le r_1 \\ (r - r_2)^2(2r + r_2 - 3r_1)/(r_2 - r_1)^3 & r_1 < r < r_2 \\ 0 & r_2 \le r \end{cases} \tag{4}$$

is multiplied to smoothly cut off the Coulomb interaction from full potential (at r_1) to zero (at r_2), where $r_1 = 8$ Å and $r_2 = 9$ Å. (Note that full Coulomb interactions are considered in later stages by the Ewald sum method, not using the switching function.)

An initial structure of the hydrogel model is obtained by inserting the prescribed number of water molecules into the structure of an appropriate density. For example, 150 water molecules and a polymer structure of PNiPAM ($x = 81$) with a density of 0.75 g/cm^3 produce an initial structure of the PNiPAM hydrogel model with water content 25 wt %. The initial structures for the systems with water contents 0, 25, and 50 wt % are obtained by the method described above. Those for the systems with a water content 75 wt % are obtained, however, by another method since degrees of polymerization are low and there is few entanglement of main chains. A polymer chain and 215 water molecules are confined directly in a unit cell under the periodic boundary condition at the density of 1.0 g/cm^3.

MD Simulation. After the steepest-descent energy minimization, MD simulations are performed at 5 temperatures (400, 350, 300, 250, 200 K). MD simulations of the first 70 000 steps at 400 K are performed under the *NVE* ensemble, and the subsequent simulations under the NPT ensemble by Nosé−Andersen method[19,20] with a constant pressure of 0.1 MPa (≃1 atm). The long-range Coulombic interactions are handled by the Ewald sum method.[14] The short-range Lennard-Jones terms of the potentials are cut off at 9 Å, and the long-range correction terms are added.[22] The other conditions, the bond length and angle constraint and the time step, are the same as in generating initial structures.

Coordinates and velocities of atoms are recorded every 20 steps on disk files for later analyses; the total sampling time amounts to 50 ps (100 000 steps) at each temperature. The sampling is made after equilibration runs of 120 000 steps (60 ps) at 400 K. The last configuration sampled at 400 K is used for an initial structure of MD runs at 350 K, and the last configuration at 350 K for an initial structure at 300 K, and so on. Between two sampling runs, an equilibration run is performed for 30 000−90 000 steps (15−45 ps), depending on temperature. During the sampling periods, the temperature and density of systems are fluctuating around average values, not shifting systematically.

MD simulations are also performed for pure water (216 molecules in a unit cell) and for the system of PVA with a water content 0.25 wt %. After simulations for pure PVA without water with stepwise lowering of temperature by a similar way to those for hydrogel models, five water molecules are inserted in the equilibrium structure at 300 K. Coordinates for 500 000 steps (250 ps) are samples after equilibration runs.

We believe that the chain statistics are achieved to some extent by the method used to obtain the initial structures. The simulation time is, however, rather short compared with relaxation time of polymer chains. Therefore, the polymer chains have not fully attained conformational equilibrium. Intramolecular hydrogen bonding and steric hindrance may alter the statistics. The present study should, however, provide many insights into characteristics of water molecules perturbed by polymer matrices.

Definition of Hydrogen Bonds. A pair of water molecules are defined to be hydrogen-bonded if distances and an angle satisfy the following conditions:

$$R_{OO} \le 3.60 \text{ Å}$$
$$R_{OH} \le 2.45 \text{ Å} \tag{5}$$
$$\phi \le 30°$$

where R_{OO} and R_{OH} are distances $O_1\cdots O_2$ and $O_1\cdots H_2$, and ϕ is an angle $O_1\cdots O_2-H_2$, where the subscripts 1 and 2 show indices of water molecules. This is the same

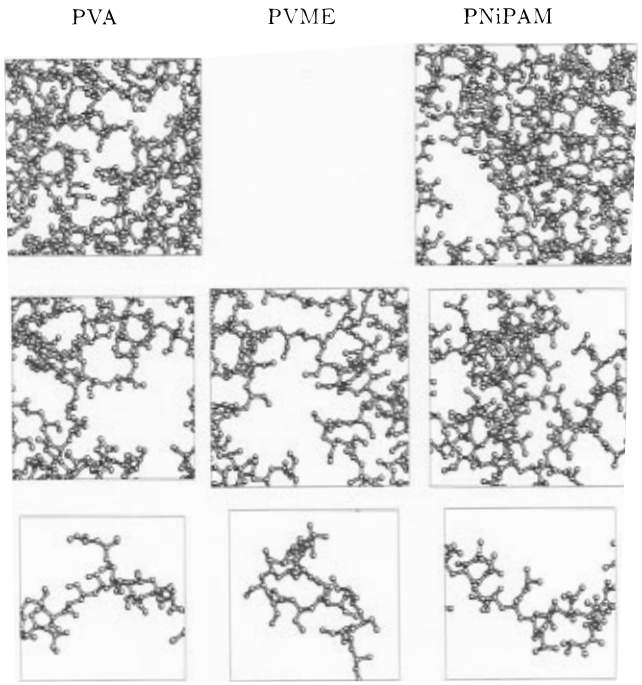

Figure 2. Snapshots of final structures of PVA, PVME, and PNiPAM hydrogel models at 300 K. No water molecules are drawn in the figure; only polymer chains are shown.

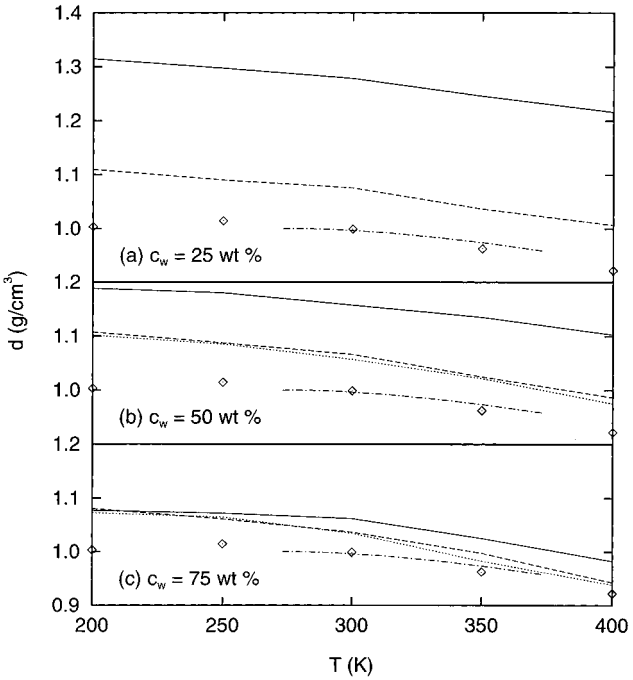

Figure 3. Temperature dependence of the densities calculated for the hydrogel models with water contents of (a) 25, (b) 50, and (c) 75 wt % and also for pure water: (solid line) PVA, (dotted line) PVME, (dashed line) PNiPAM, (dash-dot line) experimental values of pure water, (diamond) calculated values of pure water.

definition as Luzar and Chandler;[23] a schematic expression is shown in Figure 11 of their paper. The cutoff distances, R_{OO} and R_{OH}, are taken to be the distance of the first minimum in the corresponding radial distribution functions in pure water. The average number of hydrogen bonds, which increases with increase of cutoff angle ϕ, reaches an asymptotic value at $\phi \geq 30°$. They demonstrated that the number of hydrogen bonds by this definition is almost the same as that by another definition based on the pair potential energy with an appropriate threshold. The hydrophilic groups of the polymers also form hydrogen bonds to water. The hydrogen bonds are defined also for −OH of PVA and −NH− of PNiPAM in the same manner. The groups −O− of PVME and =O of PNiPAM are assumed to form the hydrogen bonds with water as a proton acceptor.

Results and Discussion

Structures. Figure 2 shows the equilibrated structure at 300 K for hydrogel models with water contents of 25, 50, and 75 wt %. The cell sizes in the figure are proportional to real cell lengths: approximately 19.6−26.3 Å. Only polymer chains are shown in the figure. For the systems of $c_w \simeq 25$ and 50 wt %, polymer chains are entangled with themselves and also with image chains. Especially for PVA, numbers of polymer−polymer hydrogen bonds are formed and the network structure is constructed by these hydrogen bonds.

For the system of $c_w \simeq 75$ wt %, the degrees of polymerization are 21 or 11, which are rather small. The end-to-end distances of the chains are approximately the same order as the unit cell lengths. Though few entanglements are observed, the chains are fairly extended and capable of interacting with the image chains; intermolecular hydrogen bonds are formed for PVA and PNiPAM.

Although no chemical cross-links are introduced in the present hydrogel models, a complicated network structure is formed by intra- and intermolecular hydrogen bonds for PVA and PNiPAM hydrogel models. Furthermore, the systems are constrained to some extent by imposing the cubic periodicity because the cell shape is fixed and the cell lengths are scaled uniformly. Therefore, we expect that the influence of cross-links is incorporated effectively on all the properties which are determined by local structures and short time scale motions.

Densities. The densities are fluctuating around average values, not shifting systematically. Figure 3 shows the temperature dependences of the average densities. For the hydrogel models, the densities are higher than those for pure water. PVME and PNiPAM models have almost the same densities, and PVA models have higher densities. The densities for PVA systems are higher with lower water contents. The dependence on water contents is smaller for PVME and PNiPAM. One of the reasons is that polymer−polymer hydrogen bonds of PVA are supposed to be more tight than those of PVME and PNiPAM. Distribution and tightness of hydrogen bonds are examined below.

The temperature dependences of densities are varied with the water contents for PVME and PNiPAM but are not for PVA. For the systems with a high water content (75 wt %), the temperature dependences are distinct for PVME and PNiPAM; the densities decrease remarkably at high temperature. Since there is no way to hold water molecules at high temperature by destruction of polymer−water hydrogen bonds, a behavior like the phase separation occurs for PVME and PNiPAM. Entanglements of polymer chains in the systems of lower water contents may diminish sharpness of the transition compared with higher water content, $c_w \simeq 75$ wt %, where a polymer chain is too short to entangle.

The calculated densities for pure water agree well with the experimental values.[24] The value for the PVA model with $c_w \simeq 0$ is 1.274 g/cm^3, which agrees well with the experimental values 1.27−1.31 g/cm^3. The densities for PVA hydrogel models with water molecules are

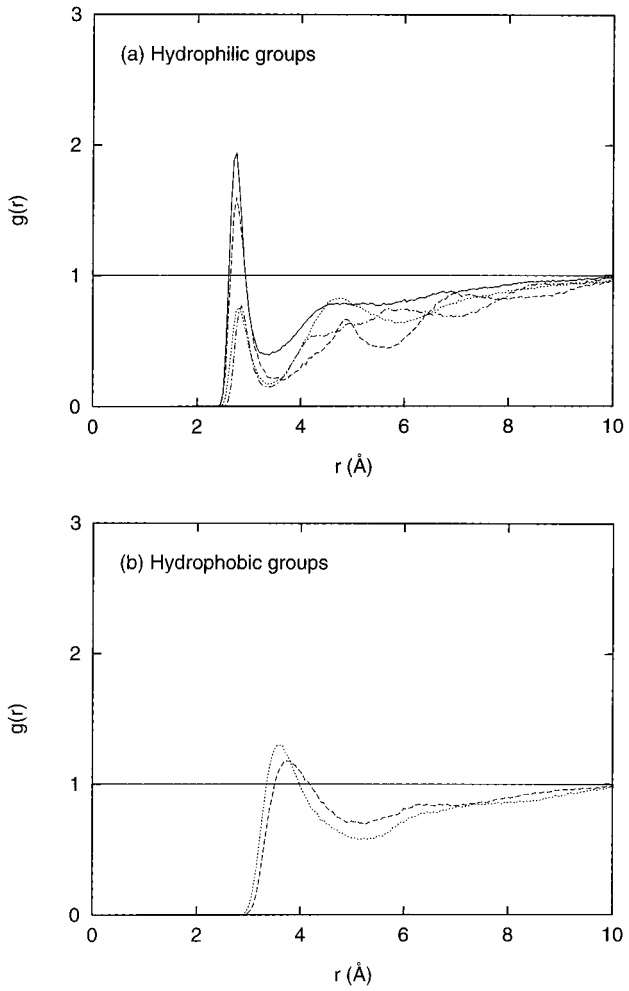

Figure 4. Radial distribution function $g(r)$ at 300 K (a) for O(water)−O(polymer) and O(water)−N(polymer) and (b) for O(water)−CH_3(polymer): (solid line) O of PVA, (dotted line) O and CH_3 of PVME, (dashed line) O and CH_3 of PNiPAM, (dash-dot line) N of PNiPAM.

distributed between those for pure water and those for pure PVA. Correct densities have been presumably reproduced by the present simulation at intermediate water content.

Radial Distribution Functions. The radial distribution functions $g(r)$ between water oxygen and functional groups of polymers are calculated. Those for the systems with a water content 50 wt % at 300 K are shown in Figures 4a and 4b, where hydrophilic and hydrophobic groups are chosen as a polymer site. The heights of the first peaks follow the order of

$$\text{O(PVA)} > \text{O(PNiPAM)} > \text{O(PVME)} \simeq \text{N(PNiPAM)}$$

PVA is the most hydrophilic among three polymers, and PVME is the least. For PVME and PNiPAM, large peaks are found in $g(r)$ around the $-CH_3$ groups, which are exposed into water. With increasing the temperature, the heights of the peaks become lower and the positions of the peaks shift slightly toward the longer distance.

Regarding the region in the first peaks of $g(r)$ as the first hydration shell, the coordination number of water molecules

$$n_{cd} = 4\pi\rho\int_0^{r_{cd}} g(r)\, r^2\, dr \qquad (6)$$

is calculated for polar groups of polymers, where ρ is the number density of water and r_{cd} is the location of the first minimum in $g(r)$. Since the temperature dependence of r_{cd} is very small, we used an fixed r_{cd} value averaged over five temperatures. The values of r_{cd} are 3.3 and 3.4 Å for oxygen and nitrogen atoms, respectively.

Table 3. Coordination Number of Water around Hydrophilic Groups of Polymers at 300 K

c_w (wt %)	O (PVA)	O (PVME)	O (PNiPAM)	N (PNiPAM)
25	1.239		0.821	0.490
50	1.526	0.536	1.042	0.510
75	2.209	1.046	1.797	0.984

Table 4. Classification of Water Molecules[a]

atom	polymer	R_{min} (Å)[b]	R_{max} (Å)
	Hydrophilic Region		
O	PVA, PVME, PNiPAM	2.40	3.30
H (OH)	PVA	1.45	2.45
H (NH)	PNiPAM	1.50	2.60
N	PNiPAM	2.60	3.40
C (CO)	PNiPAM	3.10	4.40
	Hydrophobic Region		
CH	PVA, PVME	3.00	4.10
CH	PNiPAM	3.00	4.50
CH_2	PVA, PVME, PNiPAM	3.00	4.50
CH_3	PVA, PVME, PNiPAM	3.00	4.50

[a] Spaces within R_{max} around hydrophilic and hydrophobic atoms of polymers are defined as the hydrophilic and hydrophobic regions, respectively. Each space covers the region inside the first peak of the polymer−water radial distribution function. [b] Water molecules encounter severe overlaps to host atoms within radius of R_{min}, which is only used for calculation of cluster volume of regions, and not used for classification of water molecules.

As listed in Table 3, the coordination numbers are approximately 2.2 for O (PVA), and 1 for O (PVME) and N (PNiPAM) for the systems with $c_w \simeq 75$ wt % at 300 K. An intermediate value of these two numbers, approximately 1.8, is observed for O (PNiPAM). The coordination numbers decrease at higher temperature and for the systems with smaller water contents.

Classification of Water Molecules. We classified the water molecules into three categories: (1) those around hydrophilic groups, (2) those around hydrophobic groups, and (3) the bulk region. The hydrophilic region is defined so as to cover the inner region up to the first peaks of $g(r)$ of water oxygen atoms around hydrophilic groups: −OH, −O−, and −CONH−. The hydrophobic region is similarly defined for hydrophobic groups: >CH−, $-CH_2-$, and $-CH_3$. The regions which belong to both regions (1) and (2) are incorporated in region (1). The bulk region is defined as a region outside regions (1) and (2). The other classification based on the mass center of water makes no difference. Table 4 lists the center atom species of the hydrophilic and hydrophobic regions and radii, R_{max}, of the regions around the atoms.

Table 5 lists the average number of water molecules contained in each region. The values are averaged over five temperatures from 200 to 400 K. The numbers of water molecules in the hydrophilic region follow the order of

$$\text{(PVA)} > \text{(PNiPAM)} > \text{(PVME)}$$

and those in the hydrophobic region the order of

$$\text{(PVME)} > \text{(PNiPAM)} > \text{(PVA)}$$

The orders can be accounted for by the fact that PVA is more hydrophilic and PVME is less hydrophilic. The

Table 5. Number of Water Molecules in Three Classified Regions at 300 K

c_w (wt %)	hydrophilic	hydrophobic	bulk	around O	around NH
Poly(vinyl alcohol) (PVA)					
25	111.7	23.4	14.9		
50	90.5	40.5	68.0		
75	40.6	31.8	142.6		
Poly(vinyl methyl ether) (PVME)					
50	38.7	114.4	45.9		
75	20.6	97.6	96.8		
Poly(*N*-isopropylacrylamide) (PNiPAM)					
25	71.7	71.0	7.3	52.2	36.5
50	50.2	97.6	51.2	35.5	18.1
75	29.5	76.5	109.0	18.5	10.1

numbers in the bulk region follow the order of

$$(\mathrm{PVA}) > (\mathrm{PNiPAM}) \simeq (\mathrm{PVME})$$

Since the radius from the center atom, R_{max}, is large for the hydrophobic region, the number of water molecules in the bulk region is small for PVME and PNiPAM, which have large hydrophobic side groups. The numbers in the bulk region are very small for the systems with $c_w \simeq 25$ wt %. In this water content, almost all the water molecules are highly perturbed by polymers. Most of water molecules exist in the hydrophilic region for PVA, while the numbers in the hydrophilic and hydrophobic regions are almost same for PNiPAM. As for temperature dependence, the numbers decrease in the hydrophilic and hydrophobic regions and increase in the bulk region as increasing temperature. The water molecules are extracted from the hydration shell into the bulk region at higher temperature.

Compartmentation of Water. Since water in hydrogels is highly perturbed by the polymer matrix, it has different characters from bulk water. Furthermore, water molecules are compartmentalized in hydrogels; this may lead to reduction of mobility.

To illustrate the compartmentation of water molecules, we calculate the average cluster size of each region which is continuously spread. The unit cell is divided into 100 × 100 × 100 grid points, which are classified into three regions defined above. The regions where water molecules cannot enter without severe overlaps to host atoms are excluded from the classification, referring the radial distribution functions. The excluded volume is defined as the region within R_{min} in Table 4 around host atoms. The cluster analysis is performed for the classified cubes whose centers are on the grid points in each region and whose edge lengths are equal to $^1/_{100}$ of the unit cell length. Assuming that the two classified cubes which share a surface belong to the same cluster, the clusters are constructed. Table 6 lists the volume weighted average of the cluster volume calculated for each region. Total volumes of all the clusters in each region are also listed in parentheses. As for PNiPAM, volumes separately calculated for region around =O and that around −NH− are also listed in the table.

In most regions, the average cluster volume is almost equal to the total cluster volume. A main part of each region consists of continuously spread one region. Around −O− of PVME and =O and −NH− of PNiPAM, however, differences are found between average and total cluster volumes; the classified regions consists of many small clusters. PVA has a large hydrophilic region. On the other hand, PVME and PNiPAM have widespread hydrophobic regions. As expected from Figure 2, the bulk region is percolated for the system of water content 75 wt %, while the region is compartmentalized for the system of a lower water content.

Table 6. Cluster Volume of Three Classified Regions at 300 K[a]

c_w (wt %)	hydrophilic	hydrophobic	bulk	around O	around NH
Poly(vinyl alcohol) (PVA)					
25	979 (1020)	496 (548)	507 (515)		
50	1117 (1134)	1049 (1051)	2227 (2225)		
75	515 (591)	792 (793)	4370 (4367)		
Poly(vinyl methyl ether) (PVME)					
50	23 (341)	2380 (2384)	1615 (1613)		
75	41 (225)	2062 (2061)	3169 (3164)		
Poly(*N*-isopropylacrylamide) (PNiPAM)					
25	173 (645)	1538 (1575)	334 (332)	27 (376)	8 (172)
50	317 (527)	2068 (2070)	1769 (1765)	26 (286)	7 (103)
75	388 (390)	1589 (1588)	3560 (3557)	61 (211)	12 (72)

[a] Volume weighted average in Å^3. Total volume of each region is in parentheses.

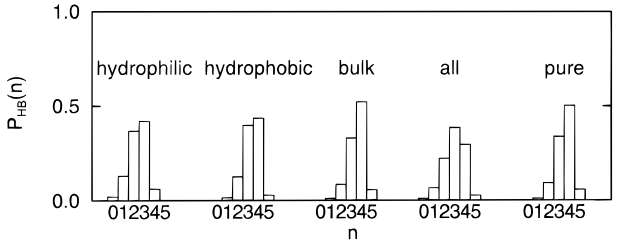

Figure 5. Hydrogen-bond number distribution, $P_{HB}(n)$, calculated for water−water hydrogen bonds at 300 K in the PVA hydrogel model with a water content 50 wt % and in pure water. The distributions are calculated for three classified regions.

Hydrogen Bond of Water. The distribution of hydrogen-bond number per atom, $P_{HB}(n)$, where n is the number of hydrogen bonds, is calculated averaging 1000 configurations for each system of $c_w \simeq 25$ and 50 wt %, and 800 configurations for each system of $c_w \simeq 75$ wt %. Figure 5 shows $P_{HB}(n)$ of water−water hydrogen bonds in each region for the system of PVA with a water content 50 wt %. In pure water, 50 % of water molecules form four hydrogen bonds. In the bulk region, the distribution is similar to those in pure water; the fraction of four hydrogen bonds is slightly larger. The fractions of three and four hydrogen bonds are almost same around hydrophobic groups. On the other hand, most of the hydrogen-bond number around hydrophilic groups is 2 or 3, which is smaller by 1 than those in pure water. Water−water hydrogen bonds are broken since hydrogen bonds are formed between water and −OH groups of PVA.

The average hydrogen-bond number, $\langle n_{HB} \rangle$, is calculated from the distribution $P_{HB}(n)$. Figure 6 shows $\langle n_{HB} \rangle$ of a water molecule in each region for the systems with $c_w \simeq 50$ wt %. Part a of Figure 6 is obtained by counting the number of hydrogen bonds of a water molecule in the hydrophilic region. The lines with squares indicate $\langle n_{HB} \rangle$ values calculated only for water−water hydrogen bonds. The other lines show $\langle n_{HB} \rangle$ for both water−water and water−polymer hydrogen bonds. The calculated values in pure water are represented by diamonds. In the hydrophilic region, $\langle n_{HB} \rangle$ values of water−water hydrogen bonds are smaller by more than 1 bond than those in pure water since water molecules form hydrogen bonds with the polymers. Around the −NH− groups of PNiPAM, the values are smaller by approximately 1.5−1.9. Including the water−polymer

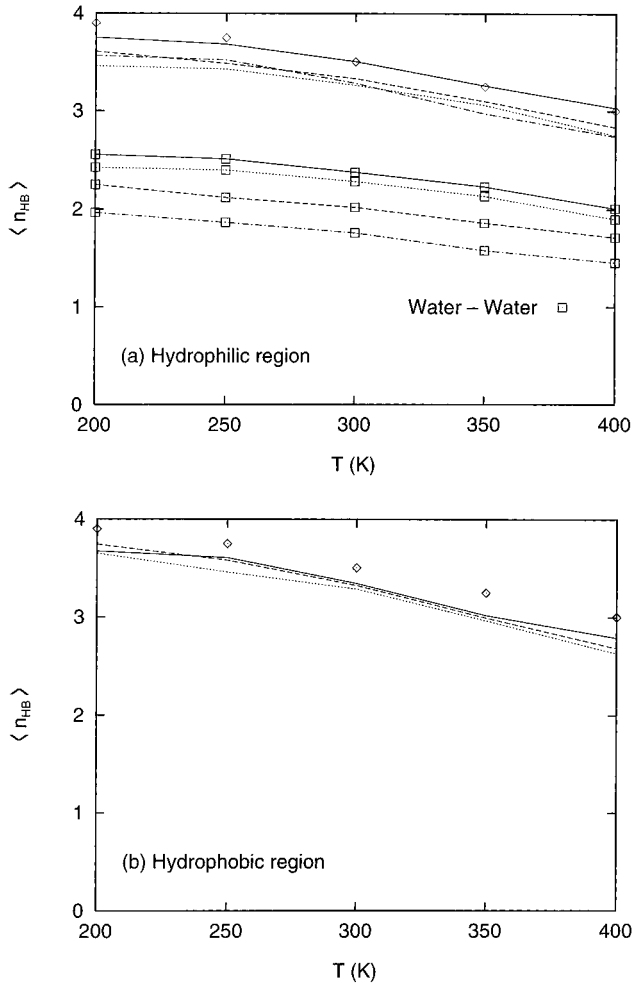

Figure 6. Average hydrogen-bond number $\langle n_{HB} \rangle$ of a water molecule (a) in the hydrophilic region and (b) in the hydrophobic region: (solid line) PVA, (dotted line) PVME, (dashed and dash-dot lines) PNiPAM, (diamond) pure water. Two lines for PNiPAM in part a show $\langle n_{HB} \rangle$ around (dashed line) =O and (dash-dot line) −NH− groups. Lines with squares indicate $\langle n_{HB} \rangle$ calculated for only water−water hydrogen bonds. Other lines show $\langle n_{HB} \rangle$ for both water−water and water−polymer hydrogen bonds.

hydrogen bonds, the total numbers of hydrogen bonds for the PVA hydrogel models are approximately equal to those in pure water. For the systems of PVME and PNiPAM hydrogel models, the numbers are slightly smaller. The defects of water−water hydrogen bonds are completely compensated by the water−polymer hydrogen bonds for PVA but not for PVME and PNiPAM.

Part b of Figure 6 is obtained by counting the number of hydrogen bonds of a water molecule in the hydrophobic region. In the region, the number of water molecules around one water molecule is smaller than that in pure water by the presence of the polymer chains. Though this leads to smaller $\langle n_{HB} \rangle$ values, the degree of the decrease is very small. Therefore, the hydrogen bonds are promoted so as to compensate for the small number of water molecules.

The values of $\langle n_{HB} \rangle$ decrease with temperature. The slopes of the lines in Figure 6 are less steep around the hydrophilic groups than those in pure water, and much steeper around the hydrophobic groups.

Though not shown in the figure, $\langle n_{HB} \rangle$ values of a water molecule in the bulk region are equal to those in pure water irrespective of polymer species and water contents. In the region out of the first hydration shell,

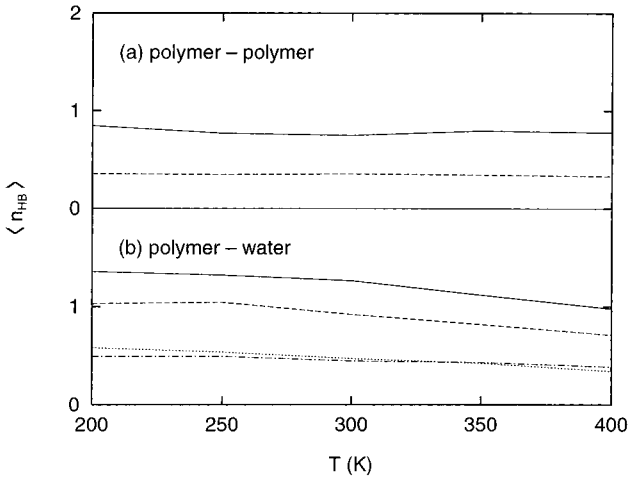

Figure 7. Average hydrogen-bond number $\langle n_{HB} \rangle$ of a hydrophilic group of polymers calculated for (a) polymer−polymer and (b) polymer−water hydrogen bonds: (solid line) PVA, (dotted line) PVME, (dashed and dash-dot lines) PNiPAM. Two lines for PNiPAM in part b show $\langle n_{HB} \rangle$ of (dashed line) =O and (dash-dot line) −NH− groups.

the hydrogen-bond numbers are not changed by polymers.

Hydrogen Bond of Polymer. Figure 7 shows $\langle n_{HB} \rangle$ of a functional group of polymers for the systems with $c_w \simeq 50$ wt %. Figure 7a shows $\langle n_{HB} \rangle$ calculated from polymer−polymer hydrogen bonds. PVA and PNiPAM forms polymer−polymer hydrogen bonds, but PVME does not. The hydrogen-bond number is approximately 0.75 for a −OH group of PVA, and 0.35 for =O and −NH− groups of PNiPAM. The temperature dependences are very small; the numbers are approximately constant.

Figure 7b shows the results calculated from polymer−water hydrogen bonds. The group −OH of PVA forms hydrogen bonds with 1.3 water molecules, and −O− of PVME and −NH− of PNiPAM with 0.5 water molecules at 300 K. The group =O of PNiPAM forms those with an intermediate number of water molecules: approximately 0.9. These values are 85−95% of the coordination numbers of each system (see Table 3). The values of $\langle n_{HB} \rangle$ decrease with increasing temperature.

It is expected that polymer−polymer hydrogen bonds are also broken at high temperature, which leads to increase in mobility of side chains. In practice, polymer−polymer hydrogen-bond numbers, however, scarcely depend on temperature. Global conformational transitions involving the whole chain are not observed. The conformation involving the polymer−polymer hydrogen bonds is scarcely changed. Even when the hydrogen bonds of side groups are broken, those are restored in a short time period.

Figure 8 shows P_{HB} ($n = 0$) for the functional groups of polymers, which is the probability that the groups form no hydrogen bonds. Figure 8a shows the results obtained from only polymer−water hydrogen bonds. For −O− of PVME and −NH− of PNiPAM, half the polar groups form no hydrogen bonds with water at 300 K. The fraction of such groups is less than 30% for −CO− of PNiPAM and less than 20% for −OH of PVA. The values of $P_{HB}(0)$ increase at high temperature; the *naked* polar groups increase with temperature. Figure 8b shows the results obtained from both polymer−water and polymer−polymer hydrogen bonds. In the case including polymer−polymer hydrogen bonds, $P_{HB}(0)$ values of PVA and PNiPAM become smaller. Most of

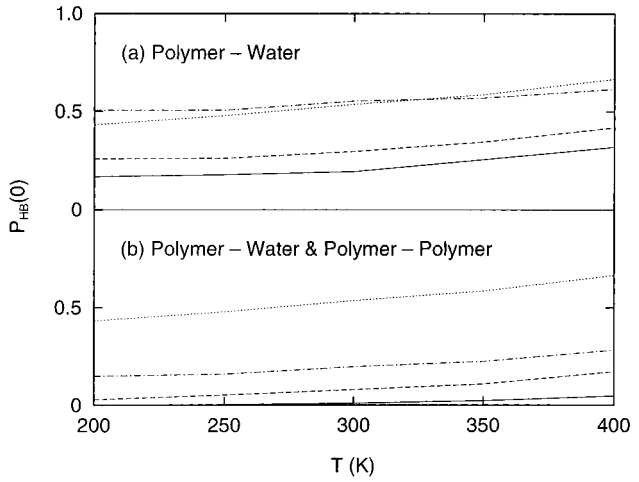

Figure 8. Non-hydrogen-bonded fraction $P_{HB}(0)$ of a hydrophilic group of polymers calculated (a) for only polymer−water hydrogen bonds and (b) for both polymer−water and polymer−polymer hydrogen bonds: (solid line) PVA, (dotted line) PVME, (dashed line) =O group of PNiPAM, (dash-dot line) −NH− group of PNiPAM.

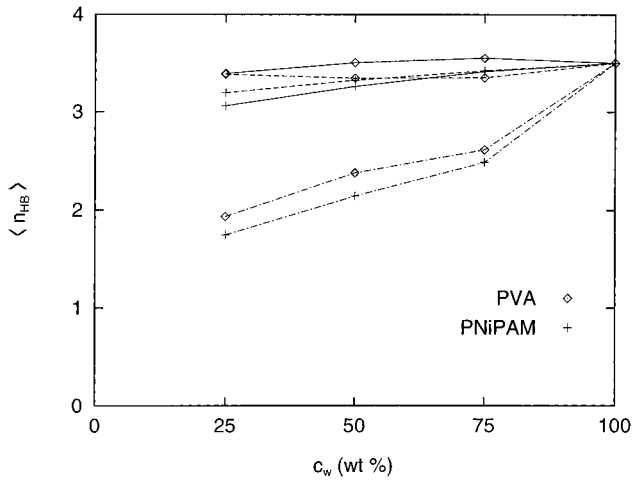

Figure 9. Average hydrogen-bond number $\langle n_{HB} \rangle$ of a water molecule plotted against water content c_w at temperature 300 K: (solid line) hydrophilic region (for both water−water and water−polymer), (dash-dot line) hydrophilic region (for only water−water), (dashed line) hydrophobic region.

the polar groups of PVA are hydrogen-bonded in all the temperature range.

PVME and PNiPAM are soluble in water at low temperature but undergo phase separation at high temperature. Even if water molecules stay inside the polymer, the so-called hydrophobic interaction[26,27] driven by the entropic contribution prevails and forces to squeeze the water molecules outside the gel and water molecules in contact with the polymer no longer stabilize it in gel form. Although the polymer−water hydrogen bonds for PVA also decrease at high temperature, the hydrophilicity is not so lowered.

Dependence on Water Content. Figure 9 shows the dependence of $\langle n_{HB} \rangle$ of water on c_w at 300 K for PVA and PNiPAM. The dash-dot lines are obtained by counting water−water hydrogen bonds in the hydrophilic region. The numbers decrease at low water contents because of the decrease in number density of water molecules and the increase in polymer−water hydrogen bonds. The numbers for PVA are larger than those for PNiPAM. The solid lines are obtained by counting both water−water and water−polymer hydrogen bonds in the hydrophilic region. The numbers also decrease at low water contents. The slope of the dependence for PNiPAM is steeper than that for PVA. The dashed lines are obtained by counting hydrogen bonds in the hydrophobic region, where the numbers also decrease at low water contents. The dependence is, however, less steep than that in the hydrophilic region. The dependence is hardly observed especially for PVA. In the bulk region, $\langle n_{HB} \rangle$ values are independent of water contents and are the same as those in pure water.

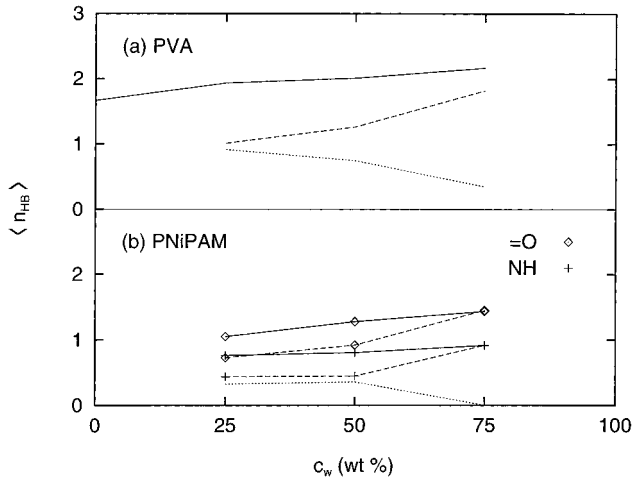

Figure 10. Average hydrogen-bond number $\langle n_{HB} \rangle$ of a hydrophilic group of polymers plotted against water content c_w: (solid line) both polymer−water and polymer−polymer, (dashed line) only polymer−water, (dotted line) only polymer−polymer hydrogen bonds.

Figure 10 shows the dependence of $\langle n_{HB} \rangle$ on c_w for polar groups of polymers at 300 K. Parts a and b of Figure 10 are those for PVA and PNiPAM, respectively. With decreasing the water contents, the numbers of polymer−polymer hydrogen bonds increase and polymer−water hydrogen bonds decrease. The total numbers of hydrogen bonds decrease at low water contents. The dependences are, however, small. For PNiPAM, the dependence of −CO− is larger than that of −NH−.

Hydrogen-Bond Defect. Defects of water−water hydrogen bonds in comparison with pure water are caused in hydrogels by the presence of polymers. The number of defects per monomer unit is defined as

$$N_D = \frac{\langle n_{HB} \rangle_w - \langle n_{HB} \rangle_g}{\langle n_{HB} \rangle_w} \times \frac{1}{f_x} \tag{7}$$

where $\langle n_{HB} \rangle_w$ and $\langle n_{HB} \rangle_g$ are average numbers of water−water hydrogen bonds per a water molecule in pure water and in hydrogel models, respectively, and f_x is the number of monomer units per one O−H group of water, which is expressed in this simulation as

$$f_x = \frac{x}{2n_w} \tag{8}$$

where x is the degree of polymerization and n_w is the number of water molecules in a unit cell.

The results are tabulated in Table 7. Clear temperature dependence is not observed. As for dependence on water contents, the numbers of water−water hydrogen bonds themselves decrease with decreasing water contents (see Figure 9), which leads to increase in the total numbers of hydrogen-bond defects. On the contrary, the defects per monomer unit, N_D, decrease

Table 7. Number of Hydrogen-Bond Defects per Monomer Unit

c_w (wt %)	av	200 K	250 K	300 K	350 K	400 K
Poly(vinyl alcohol) (PVA)						
25	0.65	0.69	0.67	0.63	0.64	0.63
50	0.77	0.85	0.79	0.75	0.76	0.70
75	1.11	1.12	1.06	1.08	1.09	1.21
Poly(vinyl methyl ether) (PVME)						
50	0.57	0.61	0.60	0.50	0.53	0.62
75	0.92	0.97	0.97	0.68	0.91	1.06
Poly(*N*-isopropylacrylamide) (PNiPAM)						
25	1.10	1.05	1.07	1.04	1.13	1.22
50	1.26	1.17	1.25	1.17	1.31	1.39
75	1.93	2.06	1.75	1.59	1.82	2.43

because the fraction of the polar groups which induce defects in water−water hydrogen bonds decreases by the increase of hydrogen bonds between two polar groups of polymers. The N_D values are small for PVME, since the number of hydrogen bonds to water is also small. The N_D values are large for PVA and PNiPAM because the numbers of hydrogen bonds to water are large and, especially, PNiPAM has two polar groups in a monomer unit.

Terada et al.[6] determined the N_D values for various hydrophilic polymers by Raman spectroscopy. The values are varied by degrees of polymerization and cross-links. The results for aqueous solutions with a water content 70 wt % at 298 K are 2.6−9.8 for cross-linked polyacrylamide (PAAm) gel, 3.2−5.1 for linear PAAm, 1−2.3 for linear poly(ethylene glycol) (PEG), etc. The experimental N_D values increase with increasing degrees of polymerization and cross-links. Our calculated values at a water content 75 wt % are smaller than the experimental values. This is probably because degrees of polymerization are small and no cross-links in our simulation. Terada et al.[6] showed that the numbers of defects in hydrophilic polymer solutions are greater than those in hydrophobic polymer solutions. This agrees qualitatively with our calculation. Maeda et al.[7] argued that the number of defects increases when the size of the cluster of *interstitial water* surrounded by polymer networks decreases below a critical size and the orientation of water molecules is restricted. Definitive evidence, however, was not obtained from our calculation.

Energy of Hydrogen Bonds. The energy of hydrogen bonds is calculated to estimate the tightness of hydrogen bonds. The nonbonded pair interaction energy is calculated for a pair of molecules which form a hydrogen bond with each other. The energy is averaged over 1000 configurations for each system. Table 8 lists the energies of water−water hydrogen bonds at 300 K in each region classified above. Average intermolecular energy in pure water is also tabulated in the table as a reference. In the bulk region, the energies are almost the same as that in pure water irrespective of polymer species and water contents. In the hydrophilic and hydrophobic regions, the energies are lower (more stable) than those in the bulk region. The stabilization of hydrogen-bond energy is very small for PVA but large for PVME and PNiPAM. Hydrogen bonds are enhanced around polymer chains most significantly for PVME, which is most hydrophobic among three polymers. The decrease in energy is significant for the systems with lower water content. The same tendency is also observed for the systems at other temperatures. Water−water hydrogen bonds are enhanced by the presence of hydrophobic groups.

Table 9 lists the energy of polymer−water and polymer−polymer hydrogen bonds. A monomer unit of polymer is treated as one group; the nonbonded pair potential energies are calculated for hydrogen-bond pairs between the group and water and between the two groups. No pairs of covalently bonded neighbor groups are included in calculating the energy between two groups of polymers. The total energy, which includes the Coulomb and the Lennard-Jones terms, is very low for PNiPAM because PNiPAM has many Lennard-Jones interaction sites (carbon atoms) in a monomer unit. The Coulomb interaction energy is determined mostly by the contribution from atoms which participate directly in the hydrogen bond. Therefore, the tightness of hydrogen bonds can be estimated based on the Coulomb interaction. The tightness of polymer−water hydrogen bonds follows the order of

$$\text{NH(PNiPAM)} > \text{OH(PVA)} > \text{CO(PNiPAM)} > \text{O(PVME)}$$

Although the −NH− group of PNiPAM has small number of hydrogen bonds, it forms the strongest hydrogen bonds. The hydrogen bonds are very tight for the −NH− group. Those for PVME are not so tight since PVME is less polar. The polymer−polymer hydrogen bonds are more tight for PNiPAM than PVA.

Comparison with Hydration in Other Systems. The behavior of water toward nonpolar solutes has long been recognized as unusual. This peculiarity and its effects are referred to as *hydrophobic effects*. The structural and thermodynamic aspects of hydrophobic effects were reviewed by Franks,[26] by Ben-Naim,[27] and more recently by Pratt.[28] The hydrophobic effect is manifest in a restructuring of the water solvent near an apolar moiety (hydrophobic hydration) and in the mutual interaction of apolar solutes in water (hydrophobic interaction). Both of these phenomena have been extensively studied through both experiments and computer simulations. Water becomes more structured and less mobile in the vicinity of these molecules. Hydrogen bonds in the vicinity of these solutes are stronger and longer lived than those in the bulk.

Pairs of nonpolar solutes in water experience an attraction with one another by the hydrophobic interaction. Semiempirical integral equation and computer simulation studies predict that for simple nonpolar solutes there exists a locally stable, solvent separated configuration of apolar solutes.[28] Such a mode of association would be particularly important if apolar moieties are unable to form contact interactions, as in the case of our system simulated.

In an aqueous solution, the presence of solutes imposes perturbations on the structure and dynamics of the solvent. The response of the system to the perturbations is the origin of solvent-induced forces (SIFs), which have been recently shown to play crucial biological roles. Brugé et al.[29,30] studied SIFs through MD simulation for aqueous solutions of a pair of simple solutes, keeping them immobilized as model groups on slowly diffusing macromolecules. According to their analysis, the water mobility around one solute strongly depends on the polarity characteristics of the other solute. When one solute in the solution of a pair of hydrophilic solutes is replaced by a hydrophobic one, the water residence time in the interior shell (region between two solutes) decreases and that in the exterior shell of the hydrophilic solute increases. This result can be related with the enhancement of the hydrogen-bond

Table 8. Energy of Water−Water Hydrogen Bonds at 300 K (kJ/mol)

	Coulomb energy			total energy		
c_w (wt %)	hydrophilic	hydrophobic	bulk	hydrophilic	hydrophobic	bulk
			Poly(vinyl alcohol) (PVA)			
25	−27.10	−27.60	−26.32	−19.69	−20.01	−19.19
50	−26.76	−26.70	−26.43	−19.64	−19.53	−19.42
75	−26.41	−26.68	−26.27	−19.46	−19.69	−19.37
			Poly(vinyl methyl ether) (PVME)			
50	−28.37	−27.23	−26.32	−21.08	−20.18	−19.35
75	−27.28	−26.90	−26.31	−20.17	−19.95	−19.40
			Poly(*N*-isopropylacrylamide) (PNiPAM)			
25	−27.31	−26.70	−26.10	−20.69	−20.06	−19.32
50	−27.43	−26.75	−26.26	−20.35	−19.89	−19.35
75	−26.52	−26.53	−26.33	−19.67	−19.68	−19.43
			Pure Water			
100			−26.21			−19.36

Table 9. Hydrogen-Bond Energy of Polymers at 300 K (kJ/mol)[a]

	Coulomb energy		total energy	
group	polymer−water	polymer−polymer[b]	polymer−water	polymer−polymer[b]
−OH (PVA)	−26.55	−26.32	−20.58	−21.53
−O− (PVME)	−20.63		−17.86	
−CO− (PNiPAM)	−24.70	−28.41	−22.34	−38.05
−NH− (PNiPAM)	−29.69		−26.13	

[a] For hydrogel models with a water content 50 wt % at 300 K. [b] Not including hydrogen bonds between neighbor segments.

network in the exterior region of hydrophilic solute as a result of a corresponding weakening in the interior shell due to presence of the hydrophobic solute.

In our present study, water−water hydrogen bonds are enhanced around hydrophobic groups especially for PVME and PNiPAM, which have methyl groups in side chain. This is owing to the hydrophobic hydration, as in the case of the hydration of a argon like particle. Hydrogen bonds are also stabilized around hydrophilic groups for PVME and PNiPAM, while not affected in the bulk region. Structure and dynamics of the hydration shell were studied through MD simulation for small molecules: alanine dipeptide[31] and crown ether 18-crown-6,[32] which contain both apolar and polar groups. Energies of water−water hydrogen bonds are stabilized around nonpolar groups while slightly unstabilized around polar ones. The differences between solvation of our systems and that of small molecules consist in finite size of the local solvent droplet, and in close packing of both nonpolar and polar species by chain connectivity, and in solvent separated contact of these species by network structure. The stability of hydrogen bonds is enhanced much more in the systems of lower water contents. One of aspects to explain this stabilization is that large hydrophobic side chains impose a constraint on the mutual orientation of water and polar group. This constraint becomes severe with decreasing the water content.

It is expected that dynamics of water is significantly perturbed by the presence of polymers. We will discuss this in the following paper.[10]

Conclusion

MD simulations have been carried out for the hydrogel models of PVA, PVME, and PNiPAM to elucidate the structure and dynamics between water and polymers. The simulations were performed for the systems with water contents 0, 25, 50, 75, and 100 wt % at five temperatures ranging from 200 to 400 K. Initial structures of polymers were obtained at very low density by the modified self-avoiding random walk method. After the structures were relaxed and compressed step by step, water molecules were inserted. We believe that the chain statistics is achieved to some extent by the method used to obtain the initial structures. The simulation time is, however, rather short compared with relaxation time of polymer chains. Therefore, the polymer chains have not fully attained conformational equilibrium. Intramolecular hydrogen bonding and steric hindrance may alter the statistics presented in this article. The present study should, however, provide insights into characteristics of water molecules perturbed by polymer matrices.

The hydrogen-bond numbers between water and polymers are the largest for PVA and the smallest for PVME. PVA is the most hydrophilic in character; only a small number of −OH groups are *naked* (not hydrogen-bonded to water).

The distributions of hydrogen bonds were analyzed for water molecules which were classified into three categories: (1) around hydrophilic groups, (2) around hydrophobic groups, and (3) the remaining bulk region. The average hydrogen-bond number $\langle n_{HB} \rangle$ was calculated for a water molecule. In the hydrophilic region, water molecules are highly perturbed by the hydrophilic groups of polymers; the values of $\langle n_{HB} \rangle$ of water−water hydrogen bonds are smaller by 1−1.9 than those in pure water. The defects of water−water hydrogen bonds are completely compensated by the water−polymer hydrogen bonds for PVA but not for PVME and PNiPAM. In the hydrophobic region, $\langle n_{HB} \rangle$ values are only slightly smaller than those in pure water, in spite of the presence of polymer chains. In the bulk region, which is far from polymers, $\langle n_{HB} \rangle$ values of a water molecule are equal to those in pure water irrespective of polymer species and water contents. In the region out of the first hydration shell, the hydrogen-bond numbers are not changed by polymers.

The water−water hydrogen bonds are stabilized in the hydrophobic region especially for PVME and PNiPAM, which have methyl groups in the side chain. This is owing to the hydrophobic hydration. Hydrogen bonds are stabilized also around hydrophilic groups for PVME and PNiPAM. The stability of hydrogen bonds is enhanced much more in the systems of lower water contents. One of aspects to explain this stabilization is that large hydrophobic side chains impose a constraint on the mutual orientation of water and polar group. This constraint becomes severe with decreasing the water content.

In this paper, static properties of hydrogen-bonded networks in hydrogels are analyzed to elucidate interplay between water and polymers. Dynamic properties of hydrogels are analyzed in the accompanying paper.[10]

Acknowledgment. Generous amounts of computer time were provided by the Computer Center, Institute for Molecular Science. Computer time was also provided by the Supercomputer Laboratory, Institute for Chemical Research, Kyoto University.

References and Notes

(1) Ohmine, I.; Tanaka, H. *Chem. Rev.* **1993**, *93*, 2545−2566.
(2) Bellissent-Funel, M.-C.; Dore, J. C., Ed. *Hydrogen Bond Networks*; Kluwer Academic Publishers: Dordrecht, The Netherlands, 1994.
(3) Ladanyi, B. M.; Skaf, M. S. *Annu. Rev. Phys. Chem.* **1993**, *44*, 335−368.
(4) Kitao, A.; Hirata, F.; Gō, N. *Chem. Phys.* **1991**, *158*, 447−472.
(5) Kitao, A.; Hirata, F.; Gō, N. *J. Phys. Chem.* **1993**, *97*, 10223−10230.
(6) Terada, T.; Maeda, Y.; Kitano, H. *J. Phys. Chem.* **1993**, *97*, 3619−3622.
(7) Maeda, Y.; Tsukida, N.; Kitano, H.; Terada, T.; Yamanaka, J. *J. Phys. Chem.* **1993**, *97*, 13903−13906.
(8) Ohta, H.; Ando, I.; Fujishige, S.; Kubota, K. *J. Polym. Sci., Polym. Phys. Ed.* **1991**, *29*, 963−968.
(9) Tamai, Y.; Tanaka, H.; Nakanishi, K. *Mol. Simul.* **1996**, *16*, 359−374.
(10) Tamai, Y.; Tanaka, H.; Nakanishi, K. *Macromolecules* **1996**, *29*, 6761−6769.
(11) Jorgensen, W. L.; Tirado-Rives, J. *J. Am. Chem. Soc.* **1988**, *110*, 1657−1666.
(12) Berendsen, H. J. C.; Grigera, J. R.; Straatsma, T. P. *J. Phys. Chem.* **1987**, *91*, 6269−6271.
(13) Weiner, S. J.; Kollman, P. A.; Case, D. A.; Singh, U. C.; Ghio, C.; Alagona, G.; Profeta, S.; Weiner, P. *J. Am. Chem. Soc.* **1984**, *106*, 765−784.
(14) Allen, M. P.; Tildesley, D. J. *Computer Simulation of Liquids*; Oxford University Press: Oxford, U.K., 1987; pp 156−162.
(15) Tamai, Y.; Tanaka, H.; Nakanishi, K. *Macromolecules* **1994**, *27*, 4498−4508.
(16) Verlet, L. *Phys. Rev.* **1967**, *159*, 98−103.
(17) Ryckaert, J. P.; Ciccotti, G.; Berendsen, H. J. C. *J. Comput. Phys.* **1977**, *23*, 327−341.
(18) Ferrario, M.; Ryckaert, J. P. *Mol. Phys.* **1985**, *54*, 587−603.
(19) Nosé, S. *J. Chem. Phys.* **1984**, *81*, 511−519.
(20) Andersen, H. C. *J. Chem. Phys.* **1980**, *72*, 2384−2393.
(21) Allen, M. P.; Tildesley, D. J. *Computer Simulation of Liquids*; Oxford University Press: Oxford, U.K., 1987.
(22) Allen, M. P.; Tildesley, D. J. *Computer Simulation of Liquids*; Oxford University Press: Oxford, U.K., 1987; pp 64−65.
(23) Luzar, A.; Chandler, D. *J. Chem. Phys.* **1993**, *98*, 8160−8173.
(24) Eisenberg, D.; Kauzmann, W. *The Structure and Properties of Water*; Oxford University Press: London, U.K., 1969.
(25) Tamai, Y.; Tanaka, H.; Nakanishi, K. *Macromolecules* **1995**, *28*, 2544−2554.
(26) Franks, F., Ed. *Water, A Comprehensive Treatise*; Plenum Press: New York, 1975; Vol. 4.
(27) Ben-Naim, A. *Hydrophobic Interactions*; Plenum Press: New York, 1980.
(28) Pratt, L. R. *Annu. Rev. Phys. Chem.* **1985**, *36*, 433−449.
(29) Brugè, F.; Fornili, S. L.; Palma-Vittorelli, M. B. *Chem. Phys. Lett.* **1996**, *250*, 443−449.
(30) Brugè, F.; Parisi, E.; Fornili, S. L. *Chem. Phys. Lett.* **1996**, *250*, 443−449.
(31) Rossky, P. J.; Karplus, M. *J. Am. Chem. Soc.* **1979**, *101*, 1913−1937.
(32) Kowall, T.; Geiger, A. *J. Phys. Chem.* **1994**, *98*, 6216−6224.

MA951635Z